Comparing potential-driven *D*BI-*i*nspired *n*on-minimal *ki*netic *c*oupling (Dinkic) inflation with observational data*

Jun Chen(陈俊)[1,2,3;1)] Wenjie Hou(侯文杰)[1,2,3;2)] Taotao Qiu(邱涛涛)[1,2;3)] Defu Hou(侯德富)[1,3;4)]

[1] Key Laboratory of Quark and Lepton Physics (MOE), Central China Normal University, Wuhan 430079, China
[2] Institute of Particle Physics, Central China Normal University, Wuhan 430079, China
[3] Institute of Astrophysics, Central China Normal University, Wuhan 430079, China

Abstract: In our previous work [1], a new kind of inflation model was proposed, which has the interesting property that its perturbation equation of motion gets a correction of k^4, due to the non-linearity of the kinetic term. Nonetheless, the scale-invariance of the power spectrum remains valid, both in large-k and small-k limits. In this paper, we investigate in detail the spectral index, the index running and the tensor/scalar ratio in this model, especially in the potential-driven case, and compare the results with the current PLANCK/BICEP observational data. We also discuss the tensor spectrum in this case, which is expected to be tested by future observations of primordial gravitational waves.

Keywords: inflation, power spectrum, gravitaional waves

PACS: 98.80.Cq **DOI:** 10.1088/1674-1137/42/4/045102

1 Introduction

With the development of the theory of inflationary cosmology, more and more interesting inflation models are being produced, with various theoretical motivations and/or observational advantages. Among them are the Galileon/Horndeski models [2–4] which have been proposed for the last few decades. In this theory, higher derivative terms and/or non-minimal couplings are included; however the interesting property is that there are no (bad) redundant dynamical degrees of freedom, which is due to the delicate design of the action.

In order to extend this theory to explore more interesting properties, constructing Beyond Horndeski models has also become popular [5–8]. In a previous study [1], one of the current authors proposed a new kind of inflation model which contains a non-minimal kinetic coupling term, and moreover, by using a DBI-type form of the action, the correction term is non-linearly included in the action. We dub this model the "DBI-inspired non-minimal kinetic coupling" (Dinkic) inflation model. This model shares the nice ghost-free property of Galileon/Horndeski models. However, there will be a correction term which is proportional to k^4 in the perturbed equation of motion, due to the non-linear form. Nevertheless, the scale invariance of the power spectrum can still be guaranteed, even in the large-k limit when this term is dominant. Due to the coupling, however, there is a deficit of the power spectrum in the large-k limit which makes the whole spectrum red-tilted.

Since observational techniques are also developing, with more and more precision and detectability, we expect to get more and more information from observational data. Apart from the most frequently used parameters, such as the amplitude of the primordial power spectrum P_ζ, the spectral index $n_{\rm s}$, and the tensor/scalar ratio r, we have also been able to detect more details of the spectrum, such as the running of the index ($\alpha_{\rm s}\equiv {\rm d}n_{\rm s}/{\rm d}\ln k$) and even the running of the running ($\beta_{\rm s}\equiv {\rm d}^2n_{\rm s}/{\rm d}\ln k^2$). For example, the PLANCK 2013 data has put stringent constraints on $\alpha_{\rm s}$: $\alpha_{\rm s}=-0.013\pm0.009$ (68% C.L.) [9], while in the PLANCK 2015 data, the constraints are improved to be $\alpha_{\rm s}=-0.0033\pm0.0074$ (68%, C.L., $\beta_{\rm s}=0$), or $\alpha_{\rm s}=0.009\pm0.010$, $\beta_{\rm s}=0.025\pm0.013$ (68%, C.L., $\beta_{\rm s}\neq0$) [10].

Besides the scalar parts, it has become more and more important to pay attention to the tensor modes of primordial perturbations, because they can generate primordial gravitational waves [11]. The recent discovery of binary gravitational waves (GW) [12] won the Nobel

Received 24 November 2017, Revised 24 January 2018, Published online 20 March 2018
* Supported by NSFC (11405069, 11653002, 11735007, 111375070)
1) E-mail: junchen@mails.ccnu.edu.cn
2) E-mail: houwenjie@mails.ccnu.edu.cn
3) E-mail: qiutt@mail.ccnu.edu.cn
4) E-mail: houdf@mail.ccnu.edu.cn
©2018 Chinese Physical Society and the Institute of High Energy Physics of the Chinese Academy of Sciences and the Institute of Modern Physics of the Chinese Academy of Sciences and IOP Publishing Ltd

Prize and was widely reported all over the world, but the next goal of detecting gravitational waves with lower frequencies is more challenging. There are many world-class projects planned for low-frequency GW, such as the eLISA satellite [13], the TianQin satellite [14], and the AliCPT telescope [15]. The AliCPT telescope (first stage), located in the Ali region of Tibet, China, at an altitude of 5,250 meters, is expected to improve the constraint on the tensor/scalar ratio to about one order of magnitude stronger within a few years. One may also be able to extract more information about tensor perturbations, such as the tensor spectral index n_T and so on [15].

In this paper, we will perform a more detailed investigation of the Dinkic inflation model, paying special attention to the case in which inflation is driven by the potential of the model. There have been many famous potential-driven inflation models such as chaotic inflation [16], natural inflation [17], new inflation [18, 19], axion monodromy inflation [20] and so on, some of which have a fundamental origin or are closely related to particle physics (for a comprehensive review see Ref. [21]). In the following, by considering various inflation potentials, we will calculate the power spectrum, spectral index and its running, and compare with the observational data. Moreover, we also consider information about tensor perturbations such as the tensor spectral index and tensor/scalar ratio, and compare them to observational constraints not only from current data, but also possible constraints from future detectors of primordial gravitational waves. Note that similar considerations for canonical inflation with non-minimal kinetic coupling were made in Ref. [22].

Our paper is organized as follows. In Section 2 we briefly review the Dinkic inflation model, and present general analytical forms of scalar and tensor spectra, spectral index and its running, as well as the tensor/scalar ratio. In Section 3, for various parameter choices of large field and small field models, we get solutions of quantities for the scalar perturbations given in Section 2, and their observational constraints. In Section 4 we discuss the tensor perturbations of these models. Section 5 contains concluding remarks.

2 The Dinkic inflation model

To start with, we write down the action of the Dinkic inflation model as [1]:

$$S=\int \mathrm{d}^4x\sqrt{-g}\left[\frac{R}{2\kappa^2}-\frac{1}{f(\phi)}(\sqrt{\mathcal{D}}-1)-V(\phi)\right], \quad (1)$$

where $\mathcal{D}\equiv 1-2\alpha f(\phi)X+2\beta f(\phi)\widetilde{X}$, with $X\equiv-\frac{1}{2}g^{\mu\nu}\partial_\mu\phi\partial_\nu\phi$ and $\widetilde{X}\equiv-\frac{1}{2M^2}G^{\mu\nu}\partial_\mu\phi\partial_\nu\phi$. M is the scale of the non-minimal kinetic coupling, while $M_{\rm pl}=\kappa^{-1}$ is the Planck scale. Note that since the kinetic coupling term $2\beta f(\phi)\widetilde{X}$ resides in the square root, the action becomes non-linear and cannot be included in the Galileon or Horndeski theories. Under the flat Friedmann-Robertson-Walker (FRW) metric ($g_{\mu\nu}=diag\{-1,a^2(t),a^2(t),a^2(t)\}$) where $X=\dot{\phi}^2/2$, $\widetilde{X}=-3(H/M)^2\dot{\phi}^2/2$, by varying the action with respect to the field ϕ, we can get the equation of motion for ϕ:

$$\begin{aligned}0 =\ & \frac{f_\phi(\sqrt{\mathcal{D}}-1)^2}{2f^2\sqrt{\mathcal{D}}}+\frac{3\beta H^2-\alpha}{\sqrt{\mathcal{D}}}\ddot{\phi}+\frac{2\beta\dot{H}+3\beta H^2-\alpha}{\sqrt{\mathcal{D}}}3H\dot{\phi}\\ &-\frac{3\beta H^2-\alpha}{2\mathcal{D}^{3/2}}\dot{\mathcal{D}}\dot{\phi}-V_\phi, \end{aligned} \quad (2)$$

and the energy density ρ and pressure p are:

$$\rho =\ \frac{(\sqrt{\mathcal{D}}-1)}{f(\phi)}+V(\phi)+\frac{\alpha\dot{\phi}^2}{\sqrt{\mathcal{D}}}+\frac{6\beta H^2\dot{\phi}^2}{M^2\sqrt{\mathcal{D}}}, \quad (3)$$

$$p =\ -\frac{(\sqrt{\mathcal{D}}-1)}{f(\phi)}-V(\phi)-\frac{3\beta H^2\dot{\phi}^2}{M^2\sqrt{\mathcal{D}}}-\left(\frac{\beta H\dot{\phi}^2}{M^2\sqrt{\mathcal{D}}}\right), \quad (4)$$

which satisfy the Friedmann equations $3H^2=\kappa^2\rho$, $\dot{H}=-\kappa^2(\rho+p)/2$. From the above equations one can see that, in the absence of the $2\beta\tilde{X}$ term and in the slow-roll limit ($\alpha f\dot{\phi}^2\ll 1$, $\sqrt{\mathcal{D}}\sim 1$), everything returns to the slow-roll canonical inflation case. In the presence of the $2\beta\tilde{X}$ term and in the slow-roll limit ($|\alpha f\dot{\phi}^2-3\beta f(H/M)^2\dot{\phi}^2|\ll 1$, $\sqrt{\mathcal{D}}\sim 1$), everything will be the same as the slow-roll canonical inflation with the kinetic term non-minimally coupled to the Einstein tensor at the background level. However, as will be shown below, due to the non-linearity of the non-minimal coupling term, the perturbation equation of motion will have a k^4-correction term which is different from its canonical correspondence. This will also cause some difference in the observables in the small scale (large k) region.

To analyse the perturbations generated by the model, we make use of the Arnowitt-Deser-Misner (ADM) formalism [23]. The perturbed action up to the second order becomes [1]:

$$\delta^2S\approx\frac{1}{2\kappa^2}\int \mathrm{d}^4xa^3\left[6\frac{x_\beta}{\mathcal{D}}\dot{\zeta}^2-\frac{2\epsilon}{a^2}(\partial\zeta)^2+\frac{16x_\beta^4y}{a^4H^2}(\partial^2\zeta)^2\right], \quad (5)$$

where $x_\beta\equiv\kappa^2\beta\dot{\phi}^2/(2M^2\sqrt{\mathcal{D}})$, $y\equiv f(\phi)M_{\rm p}^2H^2/\sqrt{\mathcal{D}}$, and $\epsilon\equiv-\dot{H}/H^2$. Moreover, to get rid of the ghost problem, x_β is required to be larger than zero.

From the action, one can easily get the perturbed equation of motion:

$$u''+c_{\rm s}^2k^2\left[1+24\frac{x_\beta^5|y|}{\epsilon^2\mathcal{D}^2}\left(\frac{c_{\rm s}k}{aH}\right)^2\right]u-\frac{z''}{z}u=0, \quad (6)$$

where $u\equiv z\zeta$, $z\equiv a\sqrt{3x_\beta/\mathcal{D}}$, $c_{\rm s}^2=\epsilon\mathcal{D}/3x_\beta$, and the prime denotes the derivative with respect to conformal time

$\tau\equiv\int a^{-1}(t)\mathrm{d}t$. The solution is:

$$u=\frac{\sqrt{\pi|\tau|}}{2}\left[H^{(1)}_{\nu}(\omega\tau)+H^{(1)}_{-\nu}(\omega\tau)\right], \tag{7}$$

with $H^{(1)}$ being the type I Hankel function, and we approximately have

$$\nu\simeq 3\int\omega\mathrm{d}\tau/(2\omega\tau),\quad \omega^2=\frac{\epsilon\mathcal{D}}{3x_\beta}\left[1+24\frac{x_\beta^5|y|}{\epsilon^2\mathcal{D}^2}\left(\frac{c_{\rm s}k}{aH}\right)^2\right]. \tag{8}$$

In the large scale limit where $k^{-1}\gg k_{\rm c}^{-1}$ by a critical k-value $k_{\rm c}\equiv aH\sqrt{\epsilon\mathcal{D}/(8x_\beta^4 y)}$, we have $\nu\simeq 3/4$, while in the small scale limit where $k^{-1}\ll k_{\rm c}^{-1}$, one has $\nu\simeq 3/2$.

The initial condition of ζ is:

$$\zeta\simeq\frac{1}{\sqrt{2\omega(k,\tau)}}\exp\left(\int^\tau\omega(k,\tau')\mathrm{d}\tau'\right),\quad\text{with}\quad\left|\frac{\omega'}{\omega^2}\right|\ll 1, \tag{9}$$

where we imposed the adiabatic (or WKB) approximation in order to keep the analogy to the usual Bunch-Davies vacuum. Note that in our case where the dispersion relationship becomes non-trivial, this approximation may not work when the variation of ω becomes robust, especially in the region between $\nu=3/4$ and $\nu=3/2$, which may affect the sub-horizon perturbations. However, from Eq. (8) one can calculate that

$$\left|\frac{\omega'}{\omega^2}\right|\simeq\frac{k\tau}{c_{\rm s}k_{\rm c}^2\tau^2[1+(k/k_{\rm c})^2]^{3/2}}. \tag{10}$$

This will be less than unity as long as $|k_{\rm c}\tau|\sim\sqrt{\epsilon\mathcal{D}/(8x_\beta^4 y)}\gg 1$, which can be easily satisfied. The cases where the WKB approximation is violated deserve further study[1)].

The super-horizon solution of Eq. (7) is

$$\zeta\simeq\frac{1}{3}\int\frac{\mathcal{D}\mathrm{d}t}{a^3(t)x_\beta}\quad\text{(large scale)}\quad\text{or}$$
$$H\sqrt{\frac{\mathcal{D}}{6x_\beta\omega^3}}\quad\text{(small scale)}, \tag{11}$$

so that in large scale limit, the power spectrum, the spectral index and the running of spectral index are:

$$P_{\rm s}^{(1)}\equiv\frac{k^3}{2\pi^2}|\zeta|^2\simeq\frac{H^2}{8\pi^2}\sqrt{\frac{3x_\beta}{\epsilon^3\mathcal{D}}}, \tag{12}$$

$$n_{\rm s}^{(1)}\equiv 1+\frac{\mathrm{d}\ln P_{\rm s}^{(1)}}{\mathrm{d}\ln k}\simeq 1-2\epsilon-\frac{3}{2}\eta+\iota-\frac{3}{4}s, \tag{13}$$

$$\alpha_{\rm s}^{(1)}\equiv\frac{\mathrm{d}n_{\rm s}^{(1)}}{\mathrm{d}\ln k}\simeq-2\eta\epsilon-\frac{3}{2}h\eta+j\iota-\frac{3}{4}\varsigma s, \tag{14}$$

respectively, where $\eta\equiv\dot\epsilon/(H\epsilon)$, $s\equiv\dot{\mathcal{D}}/(H\mathcal{D})$, $\iota\equiv\ddot\phi/(H\dot\phi)$, $h\equiv\dot\eta/(H\eta)$, $j\equiv\dot\iota/(H\iota)$, $\varsigma\equiv\dot s/(Hs)$. In the small scale limit where the k^4-term is taken into account, the power spectrum, the spectral index and the running of spectral index become:

$$P_{\rm s}^{(\rm s)}\simeq\frac{H^2}{8\pi^2}\sqrt{\frac{3x_\beta}{\epsilon^3\mathcal{D}}}\left[1-\mathcal{C}\left(\frac{c_{\rm s}k}{aH}\right)^2\right], \tag{15}$$

$$n_{\rm s}^{(\rm s)}\equiv 1+\frac{\mathrm{d}\ln P_{\rm s}^{(\rm s)}}{\mathrm{d}\ln k}\simeq 1-2\epsilon-\frac{3}{2}\eta+\iota-\frac{3}{4}s -\frac{\mathcal{C}}{1-\mathcal{C}}(5\epsilon_x+\epsilon_y-2\eta-2s), \tag{16}$$

$$\alpha_{\rm s}^{(\rm s)}\equiv\frac{\mathrm{d}n_{\rm s}^{(\rm s)}}{\mathrm{d}\ln k}\simeq-2\eta\epsilon-\frac{3}{2}h\eta+j\iota-\frac{3}{4}\varsigma s -\frac{\mathcal{C}}{(1-\mathcal{C})^2}(5\epsilon_x+\epsilon_y-2\eta-2s)^2 -\frac{\mathcal{C}}{1-\mathcal{C}}\left(-10j\iota+8\eta\epsilon-2h\eta+\iota\epsilon_f+\epsilon_f\epsilon+\frac{\epsilon_f^2}{4}\right), \tag{17}$$

where $\epsilon_x\equiv\dot x_\beta/(Hx_\beta)$, $\epsilon_y\equiv\dot y/(Hy)$, $\epsilon_f\equiv\dot f/Hf$, and $\mathcal{C}\equiv 36x_\beta^5|y|/\epsilon^2\mathcal{D}^2$. One can see that in both limits the power spectrum can be nearly scale-invariant[2)], but in the small scale limit, there is a correction to the amplitude of the power spectrum, which is due to the k^4 term correction in the expression of ω^2.

Moreover, one can also calculate the tensor perturbations by considering the tensor mode of gravitational fluctuations. The second-order action for tensor perturbations can be written as [1]:

$$\delta^2S^T=\frac{1}{8\kappa^2}\int\mathrm{d}^4xa^3\left[\mathcal{F}_{\rm T}\dot\gamma_{ij}^2-\mathcal{G}_{\rm T}\frac{(\nabla\gamma_{ij})^2}{a^2}\right], \tag{18}$$

where $\mathcal{F}_{\rm T}\equiv 1-x_\beta$, $\mathcal{G}_{\rm T}\equiv 1+x_\beta$. The equation of motion for tensor perturbation γ_{ij} is

$$\gamma_{ij}''-c_{\rm T}^2\nabla^2\gamma_{ij}+\frac{(a^2\mathcal{F}_{\rm T})'}{a^2\mathcal{F}_{\rm T}}\gamma_{ij}'=0, \tag{19}$$

where $c_{\rm T}^2\equiv\mathcal{G}_{\rm T}/\mathcal{F}_{\rm T}$. The above equation has the solution:

$$\gamma_{ij}=C_1+C_2\int\frac{\mathrm{d}t}{a^3(t)\mathcal{F}_{\rm T}}, \tag{20}$$

where C_1 and C_2 are integration constants. The power spectrum and the spectral index for tensor perturbations is

$$P_{\rm T}\equiv\frac{k^3}{2\pi^2}|\gamma_{ij}|^2=\frac{2H^2}{\mathcal{G}_{\rm T}c_{\rm T}\pi^2}, \tag{21}$$

$$n_{\rm T}\equiv\frac{\mathrm{d}\ln P_{\rm T}}{\mathrm{d}\ln k}=\frac{x_\beta}{x_\beta-1}(2\iota-s)-2\epsilon-s_{\rm T}, \tag{22}$$

where $s_{\rm T}\equiv\dot c_{\rm T}/(Hc_{\rm T})$, and with Eqs. (12) and (15), one

1) We thank the referee for pointing this out to us.

2) Although Eq. (15) contains a k^2-term which seems not to be scale-invariant, it will be compensated by the $(aH)^2$ in the denominator. This means different k-modes will exit the horizon at different times, but at the crossing point ($c_{\rm s}k=aH$) each mode has the same amplitude, and becomes constant after crossing. Similar demonstrations can also be found in Refs. [1, 24, 25].

gets the tensor/scalar ratio r as:

$$r^{(\rm l)} \equiv \frac{P_{\rm T}}{P_{\rm s}^{(\rm l)}} \simeq 16\epsilon\sqrt{\frac{\epsilon\mathcal{D}}{3x_\beta}}, \tag{23}$$

$$r^{(\rm s)} \equiv \frac{P_{\rm T}}{P_{\rm s}^{(\rm s)}} \simeq 16\epsilon\sqrt{\frac{\epsilon\mathcal{D}}{3x_\beta}}\left[1+\mathcal{C}\left(\frac{c_{\rm s}k}{aH}\right)^2\right], \tag{24}$$

for large and small scale limits, respectively.

3 Spectrum, index and its running

3.1 Slow-roll analysis in potential-driven case

In this section, we restrict ourselves to a specific case, where the inflation is driven by the potential. In this case the slow-roll approximation can be applied, and we consider the following slow-roll conditions:

$$\frac{1}{2}\alpha\dot{\phi}^2+\frac{9\beta H^2\dot{\phi}^2}{2M^2} \ll V(\phi),\ |\ddot{\phi}| \ll |3H\dot{\phi}|,\ \frac{|2\beta\dot{H}|}{|\alpha M^2+3\beta H^2|} \ll 1, \tag{25}$$

under which the equation of motion (2) and Friedmann equation are reduced to:

$$3(\alpha+\frac{3\beta H^2}{M^2})H\dot{\phi}+V_\phi \simeq 0,\ \frac{3H^2}{\kappa^2} \simeq V(\phi), \tag{26}$$

and the e-folding number N is defined as:

$$N \equiv \int_{t_*}^{t_e} H{\rm d}t = \int_{\phi_*}^{\phi_e}\frac{H}{\dot{\phi}}{\rm d}\phi \simeq -\int_{\phi_*}^{\phi_e}\frac{\kappa^2 V(\alpha M^2+\beta\kappa^2 V)}{M^2 V_\phi}{\rm d}\phi. \tag{27}$$

It is useful to define the potential-based slow-roll parameters as:

$$\begin{aligned}\epsilon_V &= \frac{M^2}{6\kappa^2}\Big(\frac{V_\phi}{V}\Big)^2\frac{(\alpha M^2+3\beta\kappa^2 V)}{(\alpha M^2+\beta\kappa^2 V)^2},\\ \eta_V &= \frac{M^2 V_{\phi\phi}}{(\alpha M^2+\beta\kappa^2 V)\kappa^2 V},\\ \xi_V^2 &= \frac{M^4 V_{\phi\phi\phi}V_\phi}{(\alpha M^2+\beta\kappa^2 V)^2\kappa^4 V^2}.\end{aligned} \tag{28}$$

In the high friction limit where $3\beta H^2 \simeq \beta\kappa^2 V \gg \alpha M^2$, one can reduce the above formulae to get: $N \simeq -\beta\kappa^4/M^2\int_{\phi_*}^{\phi_e}(V^2/V_\phi){\rm d}\phi$, $\epsilon_V \simeq M^2V_\phi^2/(2\kappa^4\beta V^3)$, $\eta_V \simeq M^2V_{\phi\phi}/(\beta\kappa^4V^2)$, $\xi_V^2 \simeq M^4V_{\phi\phi\phi}V_\phi/(\beta^2\kappa^8V^4)$, which is different from the canonical single scalar field models. By using Eq. (26), the geometry-based slow-roll parameters (ϵ, η, ι, s, h, j, ς) can be re-expressed as:

$$\begin{aligned}&\epsilon \simeq \epsilon_V,\ \ \eta \simeq 2\iota \simeq 2(3\epsilon_V-\eta_V),\ \ s \simeq 4\iota-2\epsilon \simeq 10\epsilon_V-4\eta_V,\\ &h \simeq j \simeq \frac{18\epsilon_V^2+\xi_V^2-10\epsilon_V\eta_V}{3\epsilon_V-\eta_V},\ \ \varsigma \simeq \frac{30\epsilon_V^2-18\epsilon_V\eta_V+2\xi_V^2}{5\epsilon_V-2\eta_V}.\end{aligned} \tag{29}$$

Moreover, x_β can also be expressed as $x_\beta \simeq \epsilon_V/3$. Therefore, in the large scale limit, according to Eqs. (13), (14) and (23), one can express $n_{\rm s}$, $\alpha_{\rm s}$ and r as:

$$n_{\rm s}^{(\rm l)} \simeq 1-\frac{31}{2}\epsilon_V+5\eta_V, \tag{30}$$

$$\alpha_{\rm s}^{(\rm l)} \simeq -93\epsilon_V^2+51\epsilon_V\eta_V-5\xi_V^2, \tag{31}$$

$$r^{(\rm l)} \simeq 16\epsilon_V. \tag{32}$$

In the small scale limit, some more parameters need to be taken into account. From the expressions of ϵ_x and ϵ_y, we have:

$$\epsilon_x \simeq 2\iota-\frac{1}{2}s,\quad \epsilon_y \simeq \epsilon_f-2\epsilon-\frac{1}{2}s. \tag{33}$$

Therefore, using Eqs. (16), (17) and (24), $n_{\rm s}$, $\alpha_{\rm s}$ and r turn out to be:

$$n_{\rm s}^{(\rm s)} \simeq 1-\frac{31}{2}\epsilon_V+5\eta_V+\frac{\mathcal{C}}{1-\mathcal{C}}(34\epsilon_V-14\eta_V-\epsilon_f), \tag{34}$$

$$\begin{aligned}\alpha_{\rm s}^{(\rm s)} \simeq\ & -93\epsilon_V^2+51\epsilon_V\eta_V-5\xi_V^2+\frac{\mathcal{C}}{1-\mathcal{C}}\Big(204\epsilon_V^2\\ & -124\epsilon_V\eta_V+14\xi_V^2+\eta_V\epsilon_f-4\epsilon_V\epsilon_f-\frac{\epsilon_f^2}{4}\Big)\\ & -\frac{\mathcal{C}}{(1-\mathcal{C})^2}(34\epsilon_V+14\eta_V-\epsilon_f)^2,\end{aligned} \tag{35}$$

$$r^{(\rm s)} \simeq 16\epsilon_V(1+\mathcal{C}). \tag{36}$$

One can see that, in the slow-roll approximation, these parameters of the potential-driven Dinkic inflation model can be expressed with fewer slow-roll parameters and moreover, are more analyzable. In the following, we will perform the calculation of the spectral index and its running, by taking as examples two typical cases of potential, namely the "large field potential" and the "small field potential", to see if the potential-driven Dinkic inflation model can be consistent with the observational data.

3.2 Inflation with large field potential

In the large field inflation models, the inflaton field goes from a large value towards a small value. This kind of model can usually give rise to an "attractor" behavior of inflation without fine-tuning of the initial conditions [16, 26], and also a large tensor/scalar ratio [16]. A commonly-used potential of large-field models is

$$V(\phi) = \lambda M_{\rm pl}^4(\phi/M_{\rm pl})^n,\quad n>0. \tag{37}$$

Note that for various indices n, the potential (37) can be reduced to various interesting examples. For $n=2$, Eq. (37) is reduced to the mass-squared potential ($V=m^2\phi^2/2$) where $m=\sqrt{2\lambda}/M_p$ is the mass of the inflaton field, while for $n=4$, Eq. (37) is reduced to chaotic inflation [16]. Moreover, n can even be a rational number, for example, for $n=2/3$ Eq. (37) turns into the potential of axion monodromy inflation [20] where the inflaton

field is considered to be reduced from a $D4$ brane action wrapped on a compact manifold.

From Eq. (28) and with the form of potential (37), one can get the potential-based slow-roll parameter as:

$$\epsilon_V = \frac{n^2M^2M_{\rm pl}^n}{2\beta\lambda\phi^{n+2}}, \quad \eta_V=\frac{n(n-1)M^2M_{\rm pl}^n}{\beta\lambda\phi^{n+2}},$$
$$\xi_V^2 = \frac{n^2(n-1)(n-2)M^4M_{\rm pl}^{2n}}{\beta^2\lambda^2\phi^{2n+4}}, \tag{38}$$

which are consistent with Ref. [22]. This is because the slow-roll parameters are constructed from background quantities, and as is mentioned in Section 2, the current model can be reduced to the model in Ref. [22] at background level. This is despite the perturbation quantities such as $n_{\rm s}$, $\alpha_{\rm s}$ and r being quite different, due to their difference in perturbation level, as will be shown below.

Moreover, from Eq. (27), one can get the e-folding number of inflation from the horizon-crossing to the end:

$$N=\int_{\phi_*}^{\phi_e}\left(-\frac{\beta\lambda}{n}\frac{\phi^{n+1}}{M^2M_{\rm pl}^n}\right){\rm d}\phi=\frac{\lambda\beta(\phi_*^{n+2}-\phi_e^{n+2})}{M^2M_{\rm pl}^n n(n+2)}, \tag{39}$$

where ϕ_e and ϕ_* are the values of the field when inflation ends and when the perturbation of inflation observed today begins to cross the horizon, respectively.

For $0<n<2$, ϵ_V will reach unity earlier than η_V (also shown in Ref. [22]), so we set the time when $\epsilon_V=1$ to be the ending time of inflation. Thus the final value of ϕ at the ending of inflation is obtained as:

$$\phi_e=\left[\frac{n^2M^2M_{\rm pl}^n}{2\beta\lambda}\right]^{1/(n+2)}, \tag{40}$$

and Eqs. (40) and (39) give the solution:

$$\phi_*=\left[\frac{M_{\rm pl}^nM^2n(n+2)}{\beta\lambda}\left(N+\frac{n}{2(n+2)}\right)\right]^{1/(n+2)}. \tag{41}$$

Therefore, the slow-roll parameters at the crossing point turn out to be:

$$\epsilon_{V*} = \frac{n}{2N(n+2)+n}, \tag{42}$$
$$\eta_{V*} = \frac{2(n-1)}{2N(n+2)+n}, \tag{43}$$
$$\xi_{V*}^2 = \frac{4(n-1)(n-2)}{[2N(n+2)+n]^2}, \tag{44}$$

where here and after, we use the subscript '$*$' to denote the value at the crossing time. Moreover, one has $\epsilon_{f*}=8/[2N(n+2)+n]$. From Eqs. (30)–(32) and (34)–(36), one gets the spectral index $n_{\rm s}$, its running $\alpha_{\rm s}$, and the tensor/scalar ratio r as:

$$n_{\rm s*}^{(1)} = 1-\frac{11n+20}{2[2N(n+2)+n]}, \tag{45}$$
$$\alpha_{\rm s*}^{(1)} = -\frac{(11n+20)(n+2)}{[2N(n+2)+n]^2}, \tag{46}$$
$$r_*^{(1)} = \frac{16n}{2N(n+2)+n} \tag{47}$$

for the large scale limit, and

$$n_{\rm s*}^{(\rm s)} = 1-\frac{11n+20}{2[2N(n+2)+n]}+\frac{\mathcal{C}}{1-\mathcal{C}}\frac{6n+20}{2N(n+2)+n}, \tag{48}$$
$$\alpha_{\rm s*}^{(\rm s)} = -\frac{(11n+20)(n+2)}{[2N(n+2)+n]^2}+\frac{\mathcal{C}}{1-\mathcal{C}}\frac{4(3n+10)(n+2)}{[2N(n+2)+n]^2} -\frac{\mathcal{C}}{(1-\mathcal{C})^2}\frac{4(3n+10)^2}{[2N(n+2)+n]^2}, \tag{49}$$
$$r_*^{(\rm s)} = \frac{16n(1+\mathcal{C})}{2N(n+2)+n} \tag{50}$$

for the small scale limit.

For $n\geq 2$, the inflation ends when $\eta_V=1$, which reaches unity earlier than ϵ_V. Therefore the value of ϕ at the ending of inflation can be determined as:

$$\phi_{\rm e}=\left[\frac{n(n-1)M_{\rm pl}^nM^2}{\lambda\beta}\right]^{1/(n+2)}. \tag{51}$$

Equations (51) and (39) give the solution:

$$\phi_*=\left[\frac{M_{\rm pl}^nM^2n(n+2)}{\beta\lambda}\left(N+\frac{n-1}{n+2}\right)\right]^{1/(n+2)}, \tag{52}$$

then the slow-roll parameters at the crossing point turn out to be:

$$\epsilon_{V*} = \frac{n}{2[N(n+2)+(n-1)]}, \tag{53}$$
$$\eta_{V*} = \frac{(n-1)}{N(n+2)+(n-1)}, \tag{54}$$
$$\xi_{V*}^2 = \frac{(n-1)(n-2)}{[N(n+2)+(n-1)]^2}, \tag{55}$$

and $\epsilon_{f*}=4/[N(n+2)+(n-1)]$. From Eqs. (30)-(32), one gets the spectral index $n_{\rm s}$, its running $\alpha_{\rm s}$, and the tensor/scalar ratio r as:

$$n_{\rm s*}^{(1)} = 1-\frac{11n+20}{4[N(n+2)+(n-1)]}, \tag{56}$$
$$\alpha_{\rm s*}^{(1)} = -\frac{(11n+20)(n+2)}{4[N(n+2)+(n-1)]^2}, \tag{57}$$
$$r_*^{(1)} = \frac{8n}{N(n+2)+(n-1)}, \tag{58}$$

in the large scale limit. For various choices of $n=2/3,2,4$ and $N_*=50,60$, we list the specific values of $n_{\rm s}$, $\alpha_{\rm s}$ and

r in Table 1. Moreover, from Eqs. (34)–(36), we get:

$$n_{\rm s*}^{\rm (s)} = 1-\frac{11n+20}{4[N(n+2)+(n-1)]}+\frac{\mathcal{C}}{1-\mathcal{C}}\frac{3n+10}{N(n+2)+(n-1)}, \tag{59}$$

$$\alpha_{\rm s*} = -\frac{(11n+20)(n+2)}{4[N(n+2)+(n-1)]^2}+\frac{\mathcal{C}}{1-\mathcal{C}}\frac{(3n+10)(n+2)}{[N(n+2)+(n-1)]^2} -\frac{\mathcal{C}}{(1-\mathcal{C})^2}\frac{(3n+10)^2}{[N(n+2)+(n-1)]^2} \tag{60}$$

$$r_*^{\rm (s)} = \frac{8n(1+\mathcal{C})}{N(n+2)+(n-1)} \tag{61}$$

in the small scale limit. One can see that in both limits, $n_{\rm s}$, $\alpha_{\rm s}$ and r are all functions of the power-law index of the potential n and the e-folding number N_* only.

In Fig. 1, we plot the constraint contour of $n_{\rm s}-r$ as well as $\alpha_{\rm s}-n_{\rm s}$ for each case, and compare them with the PLANCK TT+lowP+BICEP data [27]. From the $n_{\rm s}-r$ plot we can see that most of these cases fall in the (at least 2σ) confidence level of the observational data. Especially, because of the non-minimal coupling effect, the tensor/scalar ratio of power-law inflation model can be quite suppressed. The model with smaller n gives lower r and thus has a better fit to the data, which is similar to the GR case. Therefore, for $n=2/3$ with $N=60$, the model in the large scale limit can fit the data at 1σ confidence level, while $n>4$ may fall outside the 2σ region. Moreover, considering small scale can help improve the data fitting. In the $\alpha_{\rm s}-n_{\rm s}$ plot we see that neither $n_{\rm s}$ nor $\alpha_{\rm s}$ are very sensitive to the parameters, so the data points overlap with each other. For $N>50$, the data points can fall into the 1σ confidence level.

A side comment on the constraint from the Lyth bound is given here. As D. Lyth suggested in 1996 [28], a detectable r will also give rise to a super-Planckian excursion of ϕ, therefore the effective field theory description of inflation may not be trustable. However, since Ref. [28] only considered canonical large field models and assumed a monotonic slow-roll parameter, many articles [29–36] argue that for more general inflation models, this bound could be modified. In our model, using Eqs. (40), (41), (51) and (52), one can also calculate the excursion of ϕ during inflation:

$$\Delta\phi\equiv|\phi_*-\phi_{\rm e}| = \left(\frac{M^2M_{\rm pl}^n}{2\lambda\beta}\right)^{\frac{1}{n+2}}\left([2N(n+2)n+n^2]^{\frac{1}{n+2}}-n^{\frac{2}{n+2}}\right) \text{ for small } k, \tag{62}$$

$$\text{or} \quad \left(\frac{M^2M_{\rm pl}^n}{\lambda\beta}\right)^{\frac{1}{n+2}}\left([N(n+2)n+(n-1)n]^{\frac{1}{n+2}}-[n(n-1)]^{\frac{1}{n+2}}\right) \text{ for large } k. \tag{63}$$

Table 1. The large scale limit $n_{\rm s}$, $\alpha_{\rm s}$ and r for large field inflation models with various potential index n and e-folding number N.

	$N=50$			$N=60$		
	$n=2/3$	$n=2$	$n=4$	$n=2/3$	$n=2$	$n=4$
$n_{\rm s}$	0.9489	0.9477	0.9472	0.9574	0.9564	0.9559
$\alpha_{\rm s}$	-0.0010198	-0.0010395	-0.0010456	-0.0007088	-0.0007231	-0.0007285
r	0.0399	0.0796	0.1056	0.0333	0.0663	0.0881

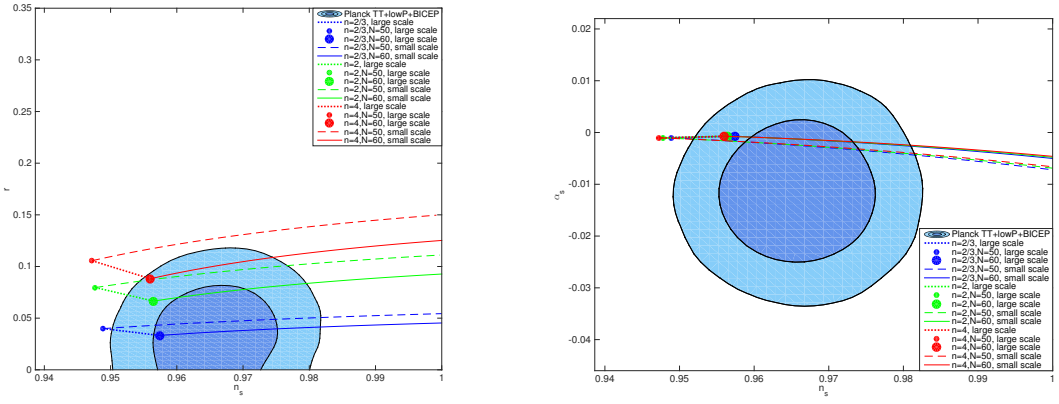

Fig. 1. (color online) Plot of $n_{\rm s}$–r (left panel) and $n_{\rm s}$–$\alpha_{\rm s}$ (right panel) of large field inflation models, with comparison to PLANCK TT+lowP+BICEP data.

From the above one can see that the field variation $\Delta\phi$ does not depend only on model parameters such as n, λ, β, M and the e-folding number N_*, some of which are not constrained by the observational data. Therefore, it is easy for $\Delta\phi<M_{\rm pl}$ to be satisfied with a proper choice of these parameters. For example, if we set the kinetic nonminimal coupling scale $M\sim10^{-6}M_{\rm pl}$, for $N=50$ inflation with $n=4$, we can get $\Delta\phi\simeq0.8M_{\rm pl}<1M_{\rm pl}$ for $\lambda=10^{-10}$ and $\beta=1$. A more general analysis can be seen for the canonical NKC inflation case in Ref. [22].

3.3 Inflation with small field potential

In the small field inflation models, the inflaton field goes in the opposite direction, namely from a small value towards a large value. Different from large field models, for small field models the initial conditions usually have to be fine-tuned, and the tensor/scalar ratio is small [26]. One possible small-field potential can be written as:

$$V(\phi)=\Lambda\left[1-\left(\frac{\phi}{v}\right)^2\right]^n. \tag{64}$$

For $|\phi/v|\ll1$, the potential will reduce to a cosmological constant, $V(\phi)\simeq\Lambda$. For different choices of n, several known models can also be recovered. For $n=1$, Eq. (64) is an example of the so-called "hill-top" potential [18] and can be used as the potential of the IR model of DBI inflation [37]. For $n=2$, Eq. (64) is nothing but the symmetry-breaking potential [19], which is applied in the Higgs-inflation scenario [38].

Considering the small-field potential Eq. (64) and with Eq. (28), one can get the potential-based slow-roll parameters as:

$$\epsilon_V = \frac{2M^2M_{\rm pl}^4}{\Lambda\beta v^2}\frac{n^2(\phi/v)^2}{[1-(\phi/v)^2]^{n+2}}, \tag{65}$$

$$\eta_V = -\frac{2M^2M_{\rm pl}^4}{\Lambda\beta v^2}\frac{n[1-(2n-1)(\phi/v)^2]}{[1-(\phi/v)^2]^{n+2}}, \tag{66}$$

$$\xi_V^2 = -\frac{24M^2M_{\rm pl}^6}{\Lambda^2\beta^2v^4}\frac{n^2(n-1)(\phi/v)^2}{[1-(\phi/v)^2]^{2n+3}} + \frac{16M^4M_{\rm pl}^8}{\Lambda^2\beta^2v^4}\frac{n^2(n-1)(n-2)(\phi/v)^4}{[1-(\phi/v)^2]^{2n+4}}. \tag{67}$$

Moreover, the e-folding number of inflation evolves from the horizon-crossing to the end, and Eq. (27) will become:

$$N = \int_{\phi_*}^{\phi_e}\frac{\Lambda\beta v^2}{2M^2M_{\rm pl}^4}\frac{[1-(\phi/v)^2]^{n+1}}{n\phi}{\rm d}\phi = -\frac{\Lambda\beta v^2}{4M^2M_{\rm pl}^4n}\left(\frac{1-[1-(\phi/v)^2]^{1+n}}{1+n} +(-1)^nB\left[\frac{v^2}{\phi^2},-n,1+n\right]\right)\Bigg|_{\phi_*}^{\phi_e}, \tag{68}$$

where $B[v^2/\phi^2,-n,1+n]$ is the incomplete beta function.

For the $n=1$ case, for a common choice of parameters such that $\Lambda=10^{-8}M_{\rm pl}^4$, $\beta=1$, $v=10M_{\rm pl}$ and $M=10^{-6}M_{\rm pl}$, one can find that ϵ_V reaches unity earlier than $|\eta_V|$, so the final value of ϕ has to be chosen at the time when $\epsilon_V=1$. However, according to Eq. (65), $\epsilon_V(\phi)=1$ is a high order algebraic equation for which it is difficult to obtain analytic solutions. We therefore turn to a numerical approach with specific values of parameters. In the above parameter choice, we find that

$$\phi_{\rm e}\simeq0.993707v=9.93707M_{\rm pl}. \tag{69}$$

Equation (68) can be simplified as:

$$N=\frac{\Lambda\beta v^2}{8M^2M_{\rm pl}^4}\left[\frac{\phi^2}{v^2}\left(\frac{\phi^2}{v^2}-4\right)+4\ln\left(\frac{\phi}{v}\right)\right]\Bigg|_{\phi_*}^{\phi_{\rm e}}, \tag{70}$$

therefore,

$$\phi_* \simeq 0.957786v=9.57786M_{\rm pl}\ (N=50), \quad \phi_* \simeq 0.955191v=9.55191M_{\rm pl}\ (N=60) \tag{71}$$

and one can immediately get $\Delta\phi\simeq0.35921M_{\rm pl}$ $(N=50)$ and $\Delta\phi\simeq0.38516M_{\rm pl}$ $(N=60)$, neither of which violate the Lyth bound. This is due to the fact that N is enhanced by a factor of M^{-2}, so in order to get proper N, less excursion of ϕ is required. By using Eqs. (65–67) as well as the definition of ϵ_f, one gets

$$\epsilon_{V*} \simeq 0.003250,\ \ \eta_{V*}\simeq-0.000293, \quad \xi_{V*}^2 \simeq 0,\ \ \epsilon_{f*}\simeq-0.001171,\quad (N=50) \tag{72}$$

$$\epsilon_{V*} \simeq 0.002714,\ \ \eta_{V*}\simeq-0.000261, \quad \xi_{V*}^2 \simeq 0,\ \ \epsilon_{f*}\simeq-0.001042,\quad (N=60) \tag{73}$$

and from Eqs. (30), (31) and (32), we get

$$n_{\rm s*}^{(\rm l)}\simeq0.948160,\ \ \alpha_{\rm s*}^{(\rm l)}\simeq-0.001031,r_*^{(\rm l)}\simeq0.052000,\ (N=50) \tag{74}$$

$$n_{\rm s*}^{(\rm l)}\simeq0.956633,\ \alpha_{\rm s*}^{(\rm l)}\simeq-0.000721,r_*^{(\rm l)}\simeq0.043424,\ (N=60) \tag{75}$$

in the large scale limit. For the small scale limit, from Eqs. (34), (35) and (36), we get

$$n_{\rm s*}^{(\rm s)} \simeq 0.948160+0.139109\frac{\mathcal{C}}{1-\mathcal{C}}, \tag{76}$$

$$\alpha_{\rm s*}^{(\rm s)} \simeq -0.001031+0.002288\frac{\mathcal{C}}{1-\mathcal{C}}-0.013403\frac{\mathcal{C}}{(1-\mathcal{C})^2}, \tag{77}$$

$$r_*^{(\rm s)} \simeq 0.052000(1+\mathcal{C}) \tag{78}$$

for $N=50$, which gives the relationship $r^{(\rm s)}=0.104000-$

$0.007234/(n_{\rm s}^{(\rm s)}-0.809051)$, and

$$n_{\rm s*}^{(\rm s)} \simeq 0.956633+0.096972\frac{\mathcal{C}}{1-\mathcal{C}}, \tag{79}$$

$$\alpha_{\rm s*}^{(\rm s)} \simeq -0.000721+0.001602\frac{\mathcal{C}}{1-\mathcal{C}}-0.009404\frac{\mathcal{C}}{(1-\mathcal{C})^2}, \tag{80}$$

$$r_*^{(\rm s)} \simeq 0.043424(1+\mathcal{C}) \tag{81}$$

for $N=60$, with the relationship $r^{(\rm s)}=0.086848-0.004211/(n_{\rm s}^{(\rm s)}-0.859661)$, respectively.

One can perform similar calculations for $n=2$. Equation (68) can be written as:

$$N=\frac{\Lambda\beta v^2}{4M^2M_{\rm pl}^4}\left[-\frac{3}{2}\left(\frac{\phi}{v}\right)^2+\frac{3}{4}\left(\frac{\phi}{v}\right)^4-\frac{1}{6}\left(\frac{\phi}{v}\right)^6+\ln\left(\frac{\phi}{v}\right)\right]\Bigg|_{\phi_*}^{\phi_e}. \tag{82}$$

For parameter choices of Λ, v and M as: $\Lambda=10^{-8}M_{\rm pl}^4$, $\beta=1$, $v=1M_{\rm pl}$, $M=10^{-6}M_{\rm pl}$, we find that $\epsilon_V=1$ can still be used as final condition of inflation, so one gets

$$\phi_e\simeq 0.915991v\simeq 0.915991M_{\rm pl}, \tag{83}$$

and

$$\begin{aligned}\phi_* &\simeq 0.674107v\simeq 0.674107M_{\rm pl}\ (N=50),\\ \phi_* &\simeq 0.658604v\simeq 0.658604M_{\rm pl}\ (N=60)\end{aligned} \tag{84}$$

and $\Delta\phi\simeq 0.241884M_{\rm pl}$ $(N=50)$ while $\Delta\phi\simeq 0.257387M_{\rm pl}$ $(N=60)$. The slow-roll parameters are

$$\begin{aligned}&\epsilon_{V*}\simeq 0.002239,\ \eta_{V*}\simeq 0.001640,\\ &\xi_{V*}^2\simeq -0.000030,\ \epsilon_{f*}\simeq -0.004926,\ (N=50)\end{aligned} \tag{85}$$

$$\begin{aligned}&\epsilon_{V*}\simeq 0.001925,\ \eta_{V*}\simeq -0.001172,\\ &\xi_{V*}^2\simeq -0.000119,\ \epsilon_{f*}\simeq -0.004407,\ (N=60)\end{aligned} \tag{86}$$

Therefore from Eqs. (30), (31) and (32), we get

$$n_{\rm s*}^{(\rm l)}\simeq 0.957096, \alpha_{\rm s*}^{(\rm l)}\simeq -0.000503, r_*^{(\rm l)}\simeq 0.035824, (N=50) \tag{87}$$

$$n_{\rm s*}^{(\rm l)}\simeq 0.964302, \alpha_{\rm s*}^{(\rm l)}\simeq 0.000135, r_*^{(\rm l)}\simeq 0.030800, (N=60) \tag{88}$$

in the large scale limit, and for the small scale limit, from Eqs. (34), (35) and (36), we get

$$n_{\rm s*}^{(\rm s)} \simeq 0.957096+0.104012\frac{\mathcal{C}}{1-\mathcal{C}}, \tag{89}$$

$$\alpha_{\rm s*}^{(\rm s)} \simeq -0.000503+0.001104\frac{\mathcal{C}}{1-\mathcal{C}}-0.010818\frac{\mathcal{C}}{(1-\mathcal{C})^2}, \tag{90}$$

$$r_*^{(\rm s)} \simeq 0.035824(1+\mathcal{C}). \tag{91}$$

for $N=50$, with the relationship $r_*^{(\rm s)}\simeq 0.071648-0.003726/(n_{\rm s*}^{(\rm s)}-0.853084)$, and

$$n_{\rm s*}^{(\rm s)} \simeq 0.964302+0.086265\frac{\mathcal{C}}{1-\mathcal{C}}, \tag{92}$$

$$\alpha_{\rm s*}^{(\rm s)} \simeq 0.000135-0.004652\frac{\mathcal{C}}{1-\mathcal{C}}-0.007442\frac{\mathcal{C}}{(1-\mathcal{C})^2}, \tag{93}$$

$$r_*^{(\rm s)} \simeq 0.030800(1+\mathcal{C}). \tag{94}$$

for $N=60$, with the relationship $r_*^{(\rm s)}\simeq 0.061600-0.002657/(n_{\rm s*}^{(\rm s)}-0.878037)$.

In Fig. 2, we plot the constraint contour of $n_{\rm s}$–r and $\alpha_{\rm s}-n_{\rm s}$ for each case, compared to the same data used for large field cases. The results are quite similar. For small field inflation, it is easier to get smaller r to fit the observational data, and for the $n=2$ case, all data points with $N\in[50,60]$ fall in the 1σ confidence level in the large scale limit. The data of $\alpha_{\rm s}$ is still not sensitive to the model parameters, and can fit with the data at 1σ confidence level.

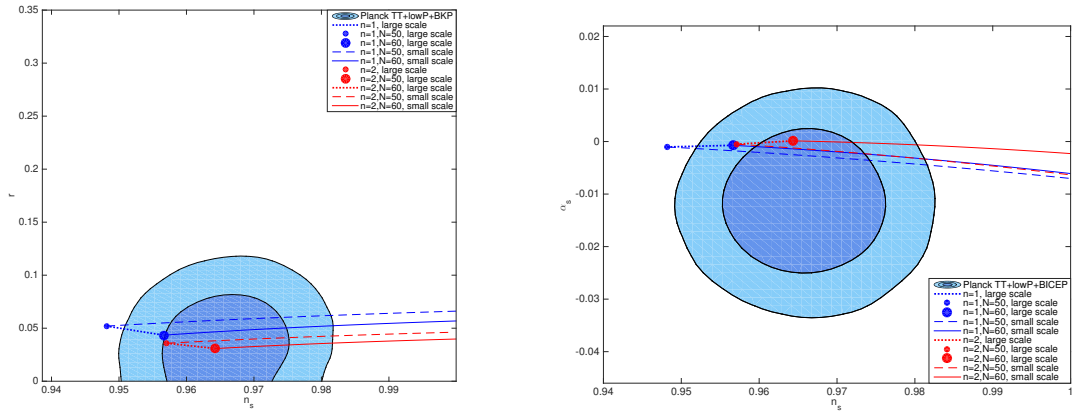

Fig. 2. (color online) Plot of $n_{\rm s}$–r (left panel) and $n_{\rm s}$–$\alpha_{\rm s}$ (right panel) of small field inflation models, with comparison to PLANCK TT+lowP+BICEP data.

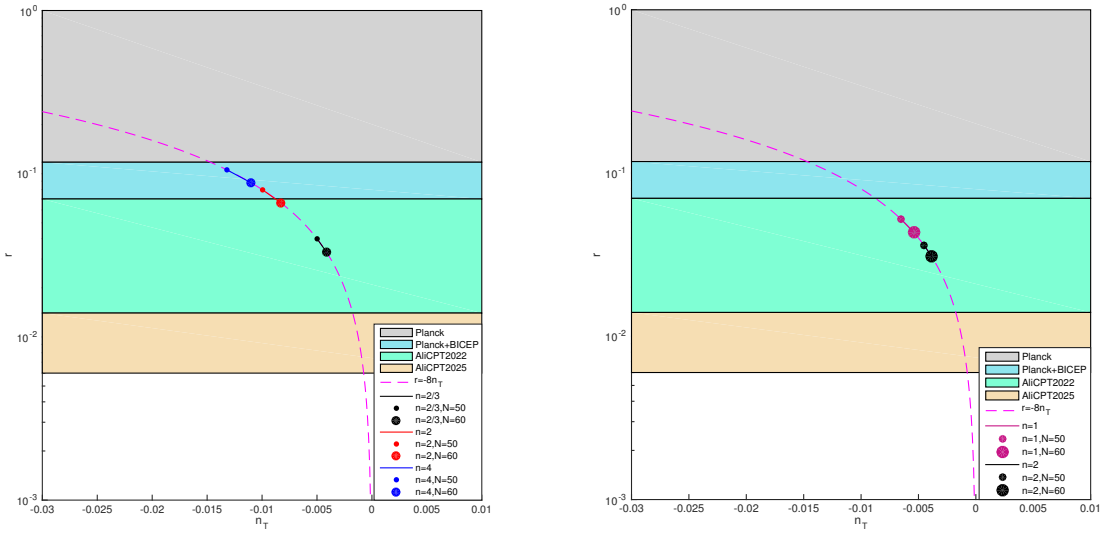

Fig. 3. (color online) $n_{\rm T}-r$ plots for large field (left panel) and small field (right panel) respectively.

4 Constraints on tensor spectrum: $n_{\rm T}$ vs. r

In this section, we analyse the relationship between spectral index for tensor perturbation $n_{\rm T}$ and the tensor/scalar ratio r in our model. The future detection capability of the AliCPT telescope in the ($n_{\rm T}$,r) parameter space has been given in Ref. [15]. In our model, one has

$$s_{\rm T}\simeq\frac{2}{3}\epsilon_V(3\epsilon_V-\eta_V), \tag{95}$$

in the potential-driven case, which is of the second order of ϵ_V, η_V, etc. Therefore, together with Eq. (29), $n_{\rm T}$ can be expressed as

$$n_{\rm T}\simeq-2\epsilon_V+\mathcal{O}(\epsilon_V^2). \tag{96}$$

At leading order, $n_{\rm T}\simeq-2\epsilon_V$. So in the large scale limit, the consistency relation of $r=-8n_{\rm T}$ can be satisfied, while in the small scale limit, it is corrected as $r=-8n_{\rm T}(1+\mathcal{C})$. However, if we go further to the second or higher orders, $n_{\rm T}$ will receive a correction from the NKC effect, and we will get a deviation from the consistency relation. Therefore, if future observations are sensitive enough to detect second order in $n_{\rm T}$, one may also tell difference between our model and minimal coupling inflation models.

In Fig. 3, we plot the relationship of ($n_{\rm T}$,r) in the large scale limit for both large and small field models, and the constraints from current Planck+BICEP data and future AliCPT predictions. The consistency relation are satisfied in both cases for the large scale limit. For large fields of $n=2$ and $n=2/3$ and for small fields of $n=1$ and $n=2$, the values of r can fall into the detectable region of the next AliCPT predictions, so one can expect to test these cases in the near future. For the small scale case, the data points will be raised due to a factor of $(1+\mathcal{C})$, with $n_{\rm T}$ unchanged.

5 Concluding remarks

In this paper, we have studied the spectral index and its running in the Dinkic inflation model, mainly focusing on the potential-driven case. In our analysis, we have taken as examples both the large field potential $V(\phi)=\lambda M_{\rm pl}^4(\phi/M_{\rm pl})^n$ and the small field potential $V(\phi)=\Lambda[1-(\phi/v)^2]^n$, with various choices of n. We have calculated the power spectrum, spectral index, the running of the index, and the tensor spectral index and tensor/scalar ratio. We have also compared our results with the observational constraints.

From the numerical plots, we can see that in the large region parameter choice, the quantities of our model can be acceptable within current observational data. Especially, the tensor/scalar ratio can be suppressed to meet with the data due to the non-minimal coupling term. The constraint on r favors smaller n for large field inflation and larger n for small field inflation, while $\alpha_{\rm s}$ is not sensitive to the model parameters in either case. Moreover, in the small scale region, there is an uncertainty due to the freedom of the parameter $\mathcal{C}$, so one can give a line rather than a point of ($n_{\rm s}$,r) and ($\alpha_{\rm s}$,$n_{\rm s}$), along which one can get some values of parameters which are favored within 1σ level for the current observational data. We also showed that at leading order, the tensor spectral index is still related to the tensor/scalar ratio with the well-known consistency relation $r=-8n_{\rm T}$, and we have

compared our results with the current and future detecting abilities of the AliCPT telescope for primordial gravitational waves.

As a final remark, we comment that due to the non-minimal kinetic term and its non-linear effect, there should be some more differences from the GR case, or even the non-minimal kinetic coupling inflation studied in [22], For example, at sub-leading order, the consistency relationship of ($n_{\rm T}$,r) can be modified. However, these differences are still very small (several orders of slow-roll parameters), and undetectable within the current observational data. We hope that future observations with higher precision and detectability can give us better distinction between different models, and a better test of our model.

We thank Ze Luan and Shulei Ni for help with plot drawing.

References

1 T. Qiu, Phys. Rev. D, **93**(12): 123515 (2016)
2 G. W. Horndeski, Int. J. Theor. Phys., **10**: 363 (1974)
3 A. Nicolis, R. Rattazzi, and E. Trincherini, Phys. Rev. D, **79**: 064036 (2009)
4 C. Deffayet, S. Deser, and G. Esposito-Farese, Phys. Rev. D, **80**: 064015 (2009) [arXiv:0906.1967 [gr-qc]]; C. Deffayet, X. Gao, D. A. Steer, and G. Zahariade, Phys. Rev. D, **84**: 064039 (2011)
5 S. A. Appleby, A. De Felice, and E. V. Linder, JCAP, **1210**: 060 (2012)
6 J. Gleyzes, D. Langlois, F. Piazza, and F. Vernizzi, Phys. Rev. Lett., **114**(21): 211101 (2015); X. Gao, Phys. Rev. D, **90**: 081501 (2014)
7 S. Ohashi, N. Tanahashi, T. Kobayashi, and M. Yamaguchi, JHEP, **1507**: 008 (2015)
8 D. Langlois and K. Noui, JCAP, **1602**(02): 034 (2016) [arXiv:1510.06930 [gr-qc]]; J. Ben Achour, D. Langlois, and K. Noui, Phys. Rev. D, **93**(12): 124005 (2016)
9 P. A. R. Ade et al (Planck Collaboration), Astron. Astrophys., **571**: A22 (2014)
10 P. A. R. Ade et al (Planck Collaboration), Astron. Astrophys., **594**: A20 (2016)
11 M. Zaldarriaga and U. Seljak, Phys. Rev. D, **55**: 1830 (1997)
12 B. P. Abbott et al (LIGO Scientific and Virgo Collaborations), Phys. Rev. Lett., **116**(6): 061102 (2016)
13 P. Amaro-Seoane et al, GW Notes, **6**: 4 (2013) [arXiv:1201.3621 [astro-ph.CO]].
14 J. Luo et al (TianQin Collaboration), Class. Quant. Grav., **33**(3): 035010 (2016)
15 H. Li et al, arXiv:1710.03047 [astro-ph.CO]
16 A. D. Linde, Phys. Lett. B, **129**: 177 (1983)
17 K. Freese, J. A. Frieman, and A. V. Olinto, Phys. Rev. Lett., **65**: 3233 (1990)
18 A. Albrecht and P. J. Steinhardt, Phys. Rev. Lett., **48**: 1220 (1982)
19 A. Albrecht and R. H. Brandenberger, Phys. Rev. D, **31**: 1225 (1985)
20 E. Silverstein and A. Westphal, Phys. Rev. D, **78**: 106003 (2008)
21 J. Martin, C. Ringeval, and V. Vennin, Phys. Dark Univ., **5-6**: 75 (2014) [arXiv:1303.3787 [astro-ph.CO]].
22 N. Yang, Q. Fei, Q. Gao, and Y. Gong, Class. Quant. Grav., **33**: no. 20, 205001 (2016)
23 R. L. Arnowitt, S. Deser, and C. W. Misner, Gen. Rel. Grav., **40**: 1997 (2008)
24 Y. F. Cai and X. Zhang, Phys. Rev. D, **80**: 043520 (2009)
25 Y. Lu and Y. S. Piao, Int. J. Mod. Phys. D, **19**: 1905 (2010)
26 R. Brandenberger, Int. J. Mod. Phys. D, **26**(01): 1740002 (2016)
27 P. A. R. Ade et al (BICEP2 and Keck Array Collaborations), Phys. Rev. Lett., **116**: 031302 (2016)
28 D. H. Lyth, Phys. Rev. Lett., **78**: 1861 (1997)
29 G. Efstathiou and K. J. Mack, JCAP, **0505**: 008 (2005)
30 I. Ben-Dayan and R. Brustein, JCAP, **1009**: 007 (2010)
31 S. Choudhury and A. Mazumdar, Nucl. Phys. B, **882**: 386 (2014)
32 S. Antusch and D. Nolde, JCAP, **1405**: 035 (2014)
33 S. Choudhury and A. Mazumdar, arXiv:1404.3398 [hep-th]
34 G. German, arXiv:1405.3246 [astro-ph.CO]
35 Q. Gao, Y. Gong, and T. Li, Phys. Rev. D, **91**: 063509 (2015)
36 M. W. Hossain, R. Myrzakulov, M. Sami, and E. N. Saridakis, Phys. Lett. B, **737**: 191 (2014)
37 X. Chen, Phys. Rev. D, **71**: 063506 (2005); X. Chen, JHEP, **0508**: 045 (2005)
38 F. L. Bezrukov and M. Shaposhnikov, Phys. Lett. B, **659**: 703 (2008)